# Combustion of Water-in-Oil Emulsion Layers Supported on Water

**A. Y. WALAVALKAR and A. K. KULKARNI***

*Department of Mechanical Engineering, The Pennsylvania State University, 333 Leonhard Building, University Park, PA 16802, USA*

In situ combustion of a water-in-oil emulsion layer supported on water is a complex process. In this paper, the combustion process of water-in-oil emulsion layers floating on top of a water body, as in the case of in situ burning of oil spilled at sea that has turned into emulsion, is modeled by using comprehensive mathematical treatment, and the results are compared with data obtained in our lab. The burning process model is divided into three regimes, as follows:

1. The initial regime begins when the emulsion layer floating on the ocean surface receives heat flux from an external source, such as an igniter or a burning oil pool;
2. The intermediate regime begins from the instant of the first appearance of an oil layer on the top of the emulsion layer due to breaking of the emulsion and continues until the oil starts to evaporate;
3. The final regime begins with the combustion of oil vapor, and ends when the fire extinguishes.

The laboratory tests were conducted: 1) to establish a critical (i.e., minimum) external heat flux value to cause self-sustaining combustion of the emulsion layer for various emulsion compositions, and 2) to generate burn rate and other emulsion pool fire characteristics, such as time for emulsion separation, burn rate, burn time, and residue volume left. Measurements were made for emulsions of commercial no. 2 diesel oil, having 20% to 80% water by volume. The model was solved numerically by using finite difference method. Predictions from the model match well with the data. 

## NOMENCLATURE

| | |
|---|---|
| $C$ | Stretching factor |
| $C_0$ | Fraction of incident heat flux not absorbed at the surface |
| $C_1$ | Inverse of oil content of emulsion, on mass basis |
| $c_{po}$ | Specific heat of oil (J/kg K) |
| $f_w$ | Fraction of water in emulsion |
| $H$ | Emulsion thickness (m) |
| $h$ | Convective heat-transfer coefficient (W/m$^2$ K) |
| $\Delta h_{v,o}$ | Heat of vaporization for oil (J/kg) |
| $\Delta h_{v,w}$ | Heat of vaporization for water (J/kg) |
| $k$ | Thermal conductivity (W/mK) |
| $L$ | Oil thickness (m) |
| $\dot{q}''$ | Incident heat flux (W/m$^2$) |
| $q_{max}$ | Maximum heat flux incident on the slick (W/m$^2$) |
| $\dot{q}''_r$ | Incident radiative heat flux (W/m$^2$) |
| $Q_{comb}$ | Energy released by combustion of oil (J/kg) |
| $Q_{Lo}$ | Energy consumed in oil vaporization (J/kg) |
| $t$ | Time (s) |
| $T_{eb}$ | Emulsion-breaking temperature (K) |
| $T$ | Temperature (K) |
| $\Delta T$ | Average temperature drop across the emulsion slick (K) |
| $U_O$ | Overall heat-transfer coefficient (W/m$^2$ K) |
| $x_e$ | Emulsion coordinates |
| $x_o$ | Oil coordinates |
| $x_w$ | Water coordinates |
| $y_w$ | Transformed water coordinates |

### Greek Symbols

| | |
|---|---|
| $\alpha$ | Thermal diffusivity (m$^2$/s) |
| $\beta$ | Inverse optical depth (m$^{-1}$) |
| $\epsilon$ | Emissivity |
| $\rho$ | Density (kg/m$^3$) |
| $\sigma$ | Stefan–Boltzmann constant ($5.67 \times 10^{-8}$ W/m$^2$ K$^4$) |

### Subscripts

| | |
|---|---|
| a | Ambient conditions |
| e | Emulsion |
| o | Oil |
| ov | Oil vaporization |
| w | Water |

*Corresponding author. E-mail: akk@psu.edu

*COMBUSTION AND FLAME* 125:1001–1011 (2001)

Published by Elsevier Science Inc.

0010-2180/01/$–see front matter
PII S0010-2180(01)00220-6

*1* Pertaining to initial regime
*2* Pertaining to intermediate regime
*3* Pertaining to final regime
i Initial conditions

## INTRODUCTION

The potential benefits of in situ burning make it one of the most effective oil-spill clean up measures. When feasible, it is an inexpensive technique, it can have a very high efficiency of removal (possibly greater than 99%), and the spill removal rate is very rapid compared to that using mechanical means. Also, emissions and ecological damage from the spill combustion have been found to be less severe compared to those from the conventional methods [1].

A review of oil spill combustion studies was presented by Walavalkar and Kulkarni [2]. The process of in situ burning of oil or water-in-oil (w/o) emulsion supported on top of a water body, such as the ocean, may be examined in three stages: before, during, and after the actual combustion. Events and considerations leading to spill combustion, which are very important in determining the efficacy of this technique as a cleanup countermeasure, include the evaporation or weathering of oil, emulsification with water, thickness of oil slick, ignition source, and surrounding conditions (including fire boom, waves, and wind conditions). The next stage is combustion of oil or emulsion, the primary focus of this paper. The processes in this stage are dominated by energy transfer to the layer, breakup of the emulsion layer, and subsequent burning of the oil layer. The final stage is characterized by the air and aquatic pollution caused by the airborne species and the residue.

## BACKGROUND

The mechanism of w/o emulsion combustion is far more complex than oil combustion. It has been postulated that it is not the emulsion that burns; rather, a layer of oil separated out of emulsion and floating on top of emulsion that burns [3]. Thus, the controlling factor in emulsion burning is the removal of water. Some experimental observations of emulsion burning reveal that: 1) incident heat helps separate water and oil in emulsion [4], and 2) burn efficiencies with emulsions, even with water content as high as 50%, are in excess of 90% [5].

The key process in sustained combustion of the oil or w/o emulsion layer on water is the energy balance at the surface. If sufficient energy from combustion is fed back to the fuel layer, the evaporation and pyrolysis of fuel continues; if excess energy is available from combustion, flame spread and more intense burning occur; and if insufficient energy is available, the fire extinguishes. Thompson et al. [6] proposed a simple energy balance for the oil layer burning on top of water:

$$\text{Net Energy} = 0.02Q_{\text{comb}} - Q_{\text{Lo}} - c_{\text{po}}(T_{\text{ov}} - T_{\text{a}})$$

Here it is assumed that 2% of heat of the combustion is returned to the fuel in order to compensate for the heat of evaporation and sensible heat.

Once the oil or emulsion layer is ignited, the sustained burn rate can be determined by examining the energy-transfer processes at the surface at steady state. A detailed analysis of combustion of oil-emulsion layer was presented by Guenette et al. [7], which was based on the work of Brzustowski and Twardus [8]. The burn rate for oil emulsions was given by:

$$r = \frac{\dot{q}''_{\text{r}} - U_0\Delta T}{\rho_{\text{o}}\Delta h_{\text{v,o}} + \rho_{\text{o}}c_{\text{po}}(T_{\text{e}} - T_{\text{a}}) - \rho_{\text{w}}\Delta h_{\text{v,w}}f_{\text{w}}/(1 - f_{\text{w}})}$$

This is a steady-state, zone model that allows computation of burn rate based on averaged quantities.

Putorti and Evans [9] carried out transient analysis of surface heating of viscous oils under external radiation flux for three heat-loss conditions at the surface. The model was limited to a pure oil layer floating on water receiving incident radiant heat flux. Ignition delay was computed under various heat flux conditions. It was concluded, after comparing the results to experiments, that the heat transfer at the surface is dominated by convective loss at the surface, and its proper accounting allowed a better prediction of ignition time.

Wu et al. [10] analyzed combustion of fuel on

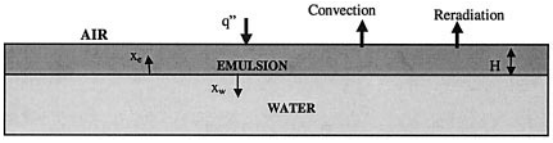


Fig. 1. Initial regime of emulsion combustion.

a water base by dividing the process into three parts, viz. ignition, flame spread, and extinction. They also extended the work of Arai et al. [11] and Garo et al. [12] to obtain an expression for average regression rate by using one-dimensional, two-layer conduction model.

The focus of the past research in this field was primarily experimental in nature. Attempts at modeling the process were limited in scope, such as zone models, or restricted to pure oil. Prior models did not predict the burning of emulsions, as they did not account for an emulsion-breaking mechanism. This paper presents a comprehensive mathematical model for the combustion of emulsion supported by a water base. The predictions of the model are compared with the experimental observations.

## PHYSICAL MODEL

In order to make the overall combustion process of an oil emulsion layer floating on top of a body of water mathematically tractable, a one-dimensional process is assumed. For modeling purposes, it is divided into three regimes as follows:

1. *Initial Regime*: ($t = 0$ to $t_1$, shown schematically in Fig. 1): The model starts with the application of external heat flux to an emulsion layer floating on top of ocean surface. Entire slick is at a uniform temperature equal to the surrounding temperature. A constant radiation heat flux source is incident on the emulsion surface. The emulsion layer is heated and eventually the top surface reaches the emulsion-breaking temperature. This marks the end of the initial regime.
2. *Intermediate Regime*: ($t = t_1$ to $t_2$, shown schematically in Fig. 2): Continued input of heat breaks the emulsion into water and oil, which causes the first appearance of oil on top of the emulsion. Thus, there are three layers in this regime, oil, emulsion, and water. The oil layer grows and the emulsion layer thins. Now the oil layer receives incident heat flux. The oil, not being optically thick, absorbs only a part of the incident heat flux at the surface and some of the radiation energy is absorbed by the oil layer. The remaining heat flux that reaches the oil-emulsion interface is absorbed at the interface. The temperature of the oil layer increases whereas the oil-emulsion interface temperature remains constant at the emulsion breaking temperature. When the oil surface temperature reaches oil vaporization temperature, the intermediate regime ends.
3. *Final Regime*: ($t = t_2$ to $t_3$, shown schematically in Fig. 3): The vaporized oil burns because of the presence of the fire, energy is released by the combustion, and a part of it is fed back to the oil. The surface temperature of the oil now stays at the oil vaporization temperature. The vaporization causes the oil layer to deplete whereas the breaking up of emulsion layer causes the oil layer to grow. The extinction of the fire may occur by one of the following two mechanisms. The combustion process continues until the emulsion layer completely breaks up and depletes, oil layer continues to burn and, finally, extinction occurs because the loss of heat (to the water and surroundings) becomes so large that not enough energy is available to cause pyrolysis of oil. The other possibility is the emulsion does not break up easily and remains stable until it reaches a high temperature and, consequently, the rate at which oil is produced

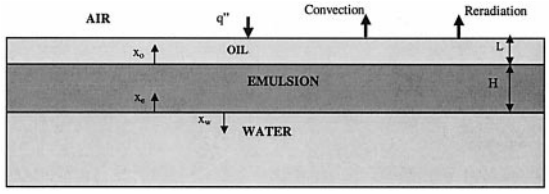


Fig. 2. Intermediate regime of emulsion combustion.

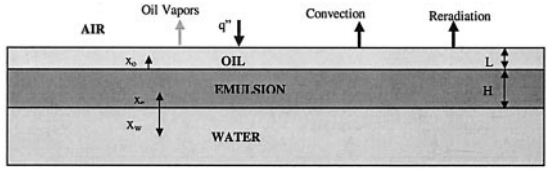


Fig. 3. Final regime of emulsion combustion.

by separating the emulsion into water and oil is slower than the rate at which oil burns. Thus, the fire can die out before all the emulsion is broken into oil and water. However, in case of diesel emulsions, the separation is complete well before the extinction occurs.

## MATHEMATICAL MODEL

*Assumptions:* The energy transfer is from the external source or igniter into the condensed phase, and in the interior of the condensed phase, it is by one-dimensional conduction. Representative properties for emulsion are assumed to be weighted averages of the corresponding oil and water properties, and constant throughout the time of operation.

When the oil begins to vaporize and burn, the incident heat flux increases rapidly to the prescribed maximum value, $q_{\max}$ (which normally depends on the type of crude oil, fire size, wind velocity, and other combustion conditions), and after that, the heat flux remains constant. Here, $q_{\max}$ is assumed to be 8 kW/m$^2$, for primarily two reasons. First, it has been known that a significant amount of flame radiation can be reflected off the oil surface depending on the incident angle, e.g., up to 60% for heptane pools at low angles [13]. The incident radiative heat flux itself varies considerably from the center to the periphery of a pool fire, e.g., for a methanol fire, it is about 15 kW/m$^2$ at center to about 2 kW/m$^2$ at the periphery, and for a heptane fire, it is about 20 kW/m$^2$ at center to about 15 kW/m$^2$ at the periphery [13]. This uncertainty lead to our estimate of 8 kW/m$^2$ as absorbed (not incident) heat flux for our experiments. Second, it yielded a reasonable burn time for one of the test conditions. Therefore, $q_{\max}$ was assumed to be 8 kW/m$^2$.

The separation of emulsion into water and oil is assumed to occur due to a sharp decrease in surface tension of water as the temperature of water approaches the boiling point. For example, surface tension of water against air decreases from 73 dynes/cm at 20°C to 63 dynes/cm at 80°C nonlinearly (with rate of reduction increasing with temperature), and then continues to fall off significantly as temperature approaches the boiling point. Accurate data for temperature dependence of water surface tension against oil used in current experiments is, however, not available. Therefore, based on experimental observations made for the diesel-water emulsions in our lab tests [14], emulsion is assumed to separate into water and oil at 90°C. (It should be noted that emulsions of some crude oils might not separate at 90°C, and in other cases the separation may occur over a range of temperature.) It is assumed that the oil separated from emulsion floats at the top and water sinks to the bottom.

The above two assumptions, namely, the heat feedback from the fire reaching a constant radiant heat flux and the separation of emulsion into water and oil occurring at a constant temperature result in significant simplification of the model. However, it will be shown later that the model successfully captures the description of the significant processes involved in emulsion combustion and thus is able to describe the experimental observations with good accuracy.

Emulsion is assumed to be optically thick, but oil is allowed in-depth absorption. This is because the emulsion is highly heterogeneous for the radiation wavelength and thus it is expected to be essentially opaque. The optical depth of oil is assumed to be 1.78 mm (Putorti and Evans [9] have reported this value for SAE 30 oil). Wind and ocean turbulence effects are neglected. Effects of aging and weathering of oil are not considered here but these effects are planned to be included in future studies.

The high viscosity of oil and very high viscosity of the emulsion (typically one or more orders of magnitude greater than that of the oil) allows an assumption of quiescent layers. The water below the emulsion is heated stably, and represents only a small amount of heat loss compared to the incident heat flux, therefore, the seawater base is modeled as a semi-infinite quiescent medium.

### Initial Regime

Governing equations:

$$\frac{\partial T_{e1}}{\partial t} = \alpha_e \frac{\partial^2 T_{e1}}{\partial x_e^2} \tag{1}$$

$$\frac{\partial T_{w1}}{\partial t} = \alpha_w \frac{\partial^2 T_{w1}}{\partial x_w^2} \tag{2}$$

Initial conditions:

$$@\ t = 0,\ T_{e1} = T_i \tag{3}$$

$$T_{w1} = T_i \tag{4}$$

Boundary conditions:

$$@\ x_e = H,\ k_e \frac{\partial T_{e1}}{\partial x_e} = \dot{q}'' - h_e(T_{e1} - T_i) - \sigma\epsilon_e(T_{e1}^4 - T_i^4) \tag{5}$$

$$@\ x_e = 0, x_w = 0,\quad k_e \frac{\partial T_{e1}}{\partial x_e} = -k_w \frac{\partial T_{w1}}{\partial x_w} \tag{6}$$

$$@\ x_w = \infty,\ T_{w1} = T_i \tag{7}$$

The initial regime ends when $T_{e1} = T_{eb}$ @ $x_e = H_i$. At the end of the initial regime, $t = t_1$, $H = H_i$.

**Intermediate Regime**

Governing equations:

$$\frac{\partial T_{o2}}{\partial t} = \alpha_o \frac{\partial^2 T_{o2}}{\partial x_o^2} + \frac{C_0 \dot{q}'' \beta e^{-\beta(L - x_o)}}{\rho_o c_{po}} \tag{8}$$

$$\frac{\partial T_{e2}}{\partial t} = \alpha_e \frac{\partial^2 T_{e2}}{\partial x_e^2} \tag{9}$$

$$\frac{\partial T_{w2}}{\partial t} = \alpha_w \frac{\partial^2 T_{w2}}{\partial x_w^2} \tag{10}$$

Initial conditions:

$$@\ t = t_1,\ T_{o2} = T_{eb} \tag{11}$$

$$T_{e2} = T_{e1} \tag{12}$$

$$T_{w2} = T_{w1} \tag{13}$$

$$L = 0 \tag{14}$$

$$H = H_i \tag{15}$$

Boundary conditions and auxiliary conditions at the boundaries:

$$@\ x_o = 0,\ T_{o2} = T_{eb} \tag{16}$$

$$@\ x_o = L,\quad k_o \frac{\partial T_{o2}}{\partial x_o} = (1 - C_o)\dot{q}'' - h_o(T_{o2} - T_i) - \sigma\epsilon_o(T_{o2}^4 - T_i^4) \tag{17}$$

$$@\ x_e = 0, x_w = 0,\quad k_e \frac{\partial T_{e2}}{\partial x_e} = -k_w \frac{\partial T_{w2}}{\partial x_w} \tag{18}$$

$$@\ x_e = H,\ T_{e2} = T_{eb} \tag{19}$$

$$@\ x_w = \infty,\ T_{w2} = T_i \tag{20}$$

$$@\ x_o = 0, x_e = H,\quad k_o \frac{\partial T_{o2}}{\partial x_o} - k_e \frac{\partial T_{e2}}{\partial x_e} = aC_0 \dot{q}'' e^{-\beta L} \tag{21}$$

The intermediate regime ends when $T_{o2} = T_{ov}$ @ $x_o = L$. At end of the intermediate regime, $t = t_2$, $H = H_2$, $L = L_2$.

**Final Regime**

Governing equations:

$$\frac{\partial T_{o3}}{\partial t} = \alpha_o \frac{\partial^2 T_{o3}}{\partial x_o^2} + \frac{C_0 \dot{q}'' \beta e^{-\beta(L - x_o)}}{\rho_o c_{po}} \tag{22}$$

$$\frac{\partial T_{e3}}{\partial t} = \alpha_e \frac{\partial^2 T_{e3}}{\partial x_e^2} \tag{23}$$

$$\frac{\partial T_{w3}}{\partial t} = \alpha_w \frac{\partial^2 T_{w3}}{\partial x_w^2} \tag{24}$$

Initial conditions:

$$@\ t = t_2,\ T_{o3} = T_{ov} \tag{25}$$

$$T_{e3} = T_{e2} \tag{26}$$

$$T_{w3} = T_{w2} \tag{27}$$

$$L = L_2 \tag{28}$$

$$H = H_2 \tag{29}$$

Boundary conditions and auxiliary conditions at the boundaries:

$$@\ x_o = 0,\ T_{o3} = T_{eb} \tag{30}$$

$$@\ x_o = L,\ T_{o3} = T_{ov} \tag{31}$$

$$@\ x_e = H,\ T_{e3} = T_{eb} \tag{32}$$

$$@\ x_e = 0, x_w = 0,\quad k_e \frac{\partial T_{e3}}{\partial x_e} = -k_w \frac{\partial T_{w3}}{\partial x_w} \tag{33}$$

$$@\ x_w = \infty,\ T_{w3} = T_i \tag{34}$$

$$@\ x_o = 0, x_e = H, k_o \frac{\partial T_{o3}}{\partial x_o}$$

$$- k_e \frac{\partial T_{e3}}{\partial x_e} = aC_0 \dot{q}'' e^{-\beta L} \quad (35)$$

$$@\ x_o = L, k_o \frac{\partial T_{o3}}{\partial x_o}$$

$$= (1 - C_o)\dot{q}'' - h_o(T_{o3} - T_i)$$

$$- \sigma \epsilon_o (T_{o3}^4 - T_i^4) - \rho_o Q_{Lo} \frac{dL}{dt} \quad (36)$$

## Numerical Solution

The emulsion layer was divided into a 0.5-mm grid for numerical computation. The oil grid spacing was calculated in such a way that one emulsion grid formed one grid length of oil after separation. Thus the oil grid spacing was a function of the fraction of oil present in the emulsion. The grid for the water base was stretched to accommodate the semi-infinite medium by using coordinate transformation. The original semi-infinite region was transformed to a finite region in the transformed coordinate system. The transformation rule used was:

$$y_w = 1 - \frac{1}{1 + Cx_w}, \quad (37)$$

Here $y_w$ is the transformed coordinate in water domain and $C$ is the stretching factor, assumed to be 0.8.

An explicit time-accurate finite difference scheme with pseudo-time stepping was used to solve the resulting set of simultaneous partial differential equations and the boundary and auxiliary conditions. A general partial differential equation selected for finite differencing can be represented as:

$$\frac{\partial T}{\partial \tau} + \frac{\partial T}{\partial t} = \alpha C_{t1} \frac{\partial^2 T}{\partial x^2} + C_{t2} \frac{\partial T}{\partial x} + \frac{aC_0 \dot{q}'' \beta e^{-\beta(L-x)}}{\rho_o c_{po}} \quad (38)$$

where, $C_{t1} = C^2(1 - x)^4$ and $C_{t2} = -4\alpha_w C^2(1 - x)^3$ for the water base and $C_{t1} = 1$ and $C_{t2} = 0$ for the oil and emulsion layers. Also, $a = 1$ for the oil layer to account for the in-depth radiation absorption and $a = 0$ for emulsion. The pseudo-time ($\tau$) derivative added to the governing equation is driven to zero by attaining steady state in pseudo-time, for each time step in real time ($t$), thus assuring a converged solution. Two-point difference in time and central difference in space is used. The code was compiled and run on SGI Irix 6.2 system. Typical run time for the code was around 20 min.

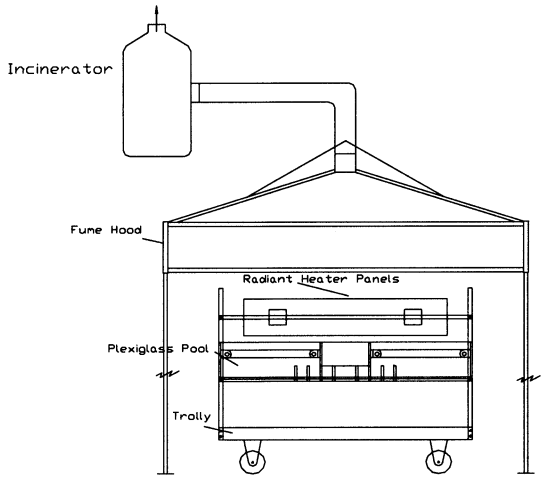


Fig. 4. Schematic of the pool fire set-up.

## EXPERIMENTS

The experimental setup was designed and instrumented to take data from pool fires of water-in-oil emulsions floating on top of water. The schematic of the pool fire setup is shown in Fig. 4. A 28 × 28 cm size pool was made in the center of a 150 × 120 × 25 cm deep, water pool. The center pool, consisting of a sheet-metal box, was supported inside the outer pool by metal bars. The water-in-oil emulsion was poured in the center pool to a desired height on top of the water to produce a 15-mm-thick fuel layer. For visual accessibility to the fire, the outer tank was made of clear acrylic. Two electrically operated heating panels (440 V, 60 amp) were used to supply external radiation. The panels were controlled by silicon control rectifiers, which allowed the panels to reach a maximum temperature of 815°C that produced a maximum radiative heat flux of about 60 kW/m$^2$ at the

panels. The panels were mounted facing toward the pool at an angle to irradiate the emulsion pool with a relatively uniform heat flux. Ignition of the pool was achieved by using long matchsticks supported at the front end of a wooden rod. Type K thermocouples were used to monitor the in-depth temperature distribution and the temperature at the oil-water interface. A video camera was used to record the test runs.

In order to aid emulsification of diesel, 10% by volume of SAE 30 oil was added [15]. The diesel content of the emulsion was varied from 20% to 80% by volume. In a typical test run, a predetermined amount of emulsion was poured evenly over the center section of the water in the pool fire set-up shown in Fig. 4. The sample was heated at a known heat flux setting. After the surface temperature reached a certain preset value, an attempt was made to ignite the sample. Upon failure to cause ignition, the heat flux level of the panels was increased by a small amount. The process was continued until sustained combustion was obtained, and the critical (i.e., minimum) heat flux needed to ignite the sample was noted. When the fire extinguished, the volume of the residue was measured. Based on the initial volume of emulsion poured and the total time of the burn, an average burn-rate value was calculated.

## RESULTS

For solving the model numerically, various property data values were required. Table 1 lists all the property values used as input to the numerical solution of the mathematical model. The diesel properties were obtained from Refs. 16 and 17.

Figure 5 shows the variation of the critical heat flux value required to cause the sustained combustion of the emulsion as a function of the water content of the emulsion. The heat flux value plotted is the average heat flux incident on the surface of the emulsion pool. The error bars indicate a variation of ±5% from the average heat flux value at the surface. The critical heat flux necessary to cause sustained fire increases with increasing water content of the emulsion.

The critical heat flux values were then used as input to the numerical solution of the mathematical model described earlier. Table 2 shows results of the lab scale burn experiments and the corresponding results from the model. These results were obtained at the external heat flux value equal to the critical heat flux. As described earlier, 90°C was used as the emulsion separation temperature, and the time it took for the top surface of the emulsion to reach 90°C was noted. This period is related to the ignition delay because the ignition occurs soon after the oil starts to vaporize. However, ignition delay itself is not calculated, nor measured, because the ignition delay is very hard to define precisely in the present setup. It will be somewhat dependent upon the position of igniter (because the process is not strictly one-dimensional) and the

**TABLE 1**

Property Value Input for the Mathematical Model

| | Property | Value |
|---|---|---|
| Commercial no. 2 diesel oil | $h_o$ | 10.0 W/m$^2$ K |
| | $\epsilon_o$ | 0.50 |
| | $k_o$ | 0.1169 W/mK |
| | $\alpha_o$ | $76.77 \times 10^{-9}$ m$^2$/s |
| | $\rho_o$ | 846 kg/m$^3$ |
| | $c_{po}$ | 1800.0 kJ/kg K |
| | $Q_{Lo}$ | $3.3 \times 10^5$ J/kg |
| | $Q_{comb}$ | $4.187 \times 10^7$ J/kg |
| | $T_{ov}$ | 112.0°C |
| | $\beta$ | 560.0 m |
| Sea water | $k_w$ | 0.67 W/mK |
| | $\alpha_w$ | $15.73 \times 10^{-6}$ m$^2$/s |
| | $\rho_w$ | 958.0 kg/m$^3$ |
| | $c_{pw}$ | 4217.0 J/kg K |
| Emulsion | $h_e$ | 10.0 W/m$^2$ K |
| | $\epsilon_e$ | 0.95 |

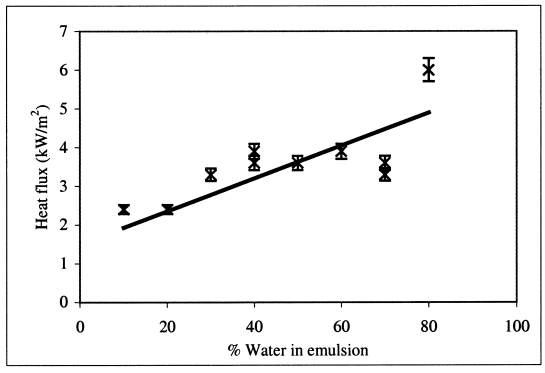


Fig. 5. Critical heat flux required to cause sustained fire as a function of water content of diesel-water emulsion.

**TABLE 2**

Comparison of Model Predictions with Experimental Data

| % Water | Figure 6 | | Figure 7 | | Figure 9 | | Figure 10 | | Figure 11 | |
|---|---|---|---|---|---|---|---|---|---|---|
| | Time for emulsion separation at critical heat flux (s) | | Time for emulsion separation at a constant heat flux of 8 kW/m$^2$ (s) | | Average burn rate (mm/s) | | Burn time (s) | | Oil residue thickness (mm) | |
| | Exptl | Model | Exptl | Model | Exptl | Model | Exptl | Model | Exptl | Model |
| 20 | | 540 | 65 | 37 | 0.010723 | 0.0123 | 746 | 695 | 3.50 | 3.48 |
| 30 | 600 | 350 | 65 | 53 | 0.009447 | 0.0118 | 765 | 651 | 2.81 | 2.80 |
| 40 | 430 | 375 | 87 | 68 | 0.009613 | 0.0098 | 612 | 578 | 2.59 | 3.32 |
| 50 | 440 | 470 | 87 | 90 | 0.007969 | 0.0115 | 475 | 439 | 2.97 | 2.44 |
| 60 | | | | | 0.007224 | 0.0098 | 405 | 361 | 2.31 | 2.48 |
| 70 | | | | | 0.007406 | 0.0099 | 244 | 240 | 1.79 | 2.13 |
| 80 | | | | | 0.020626 | 0.0099 | 106 | 129 | 0.41 | 1.72 |

"flashing" phenomenon occurring before sustained ignition. Two different values of time for separation are reported in the table below, one is calculated at the critical heat flux value (which depends on the percent water content) and the other at a fixed external heat flux value equal to 8 kW/m$^2$. The plots of these results are shown in Figs. 6–11.

The overall uncertainty in the experimental values is best indicated by the scatter in the data. It is estimated to be about 4% for the burn-time measurements, 11% for the residue thickness measurements and 9% for the burn-rate measurements. The critical heat flux values are estimated to have an uncertainty of about $\pm 0.3$ kW/m$^2$ in addition to a nonuniformity of $\pm 5\%$ around the mean values reported.

Figures 6 and 7 show the time for emulsion separation as a function of water content of the emulsion at the critical heat flux and at a constant incident heat flux of 8 kW/m$^2$, respectively. It can be seen that the model predictions show a trend similar to that of the experimental observations in Fig. 7. However, in Fig. 6, model results and predictions do not agree so well. It is because at the critical heat flux, the "flashing" phenomenon is much more prominent and it affects the estimation of the separation time significantly (even with the definition of reaching 90°C at the surface), particularly at the lower critical heat flux values (i.e., at the low water content).

At a constant external heat flux, time for emulsion separation increases with increasing water content of the emulsion. This is because, as the water fraction of emulsion increases, the thermal diffusivity of the emulsion layer increases. This means that the emulsion layer is now conducting more of the heat received. Thus, it takes more time for the surface temperature to reach the emulsion-breaking temperature.

Figure 8 shows the temperature variation inside the pool as a function of distance from the pool surface at various time intervals from start of heating. Continuous lines represent the profiles obtained from the model, and the tem-

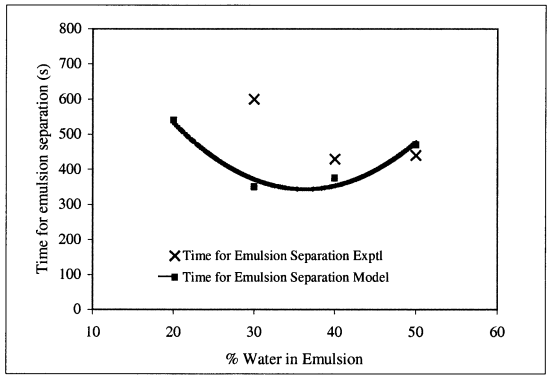


Fig. 6. Comparison of model prediction of time for emulsion separation with the experimentally observed values of time for emulsion separation as a function of water content of the emulsion at *critical heat flux*.

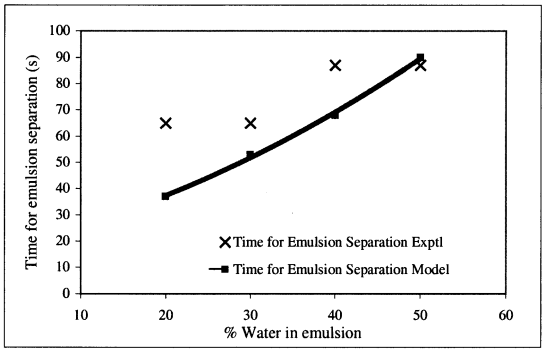


Fig. 7. Comparison of model prediction of time for emulsion separation with the experimentally observed values of time for emulsion separation as a function of water content of the emulsion at a *constant heat flux of 8 kW/m²*.

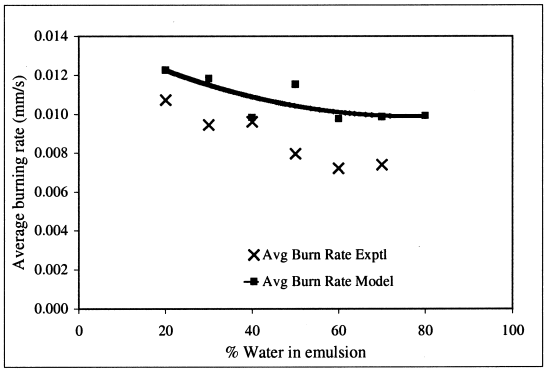


Fig. 9. Comparison of average diesel burning rate predicted by the model with the experimental average diesel burning rate values as a function of water content of the emulsion at critical heat flux.

perature values measured during the experiments are indicated by symbols. The data presented are for 50% water in diesel emulsion heated by using heat flux of 3.6 kW/m$^2$.

The following three figures are presented for important experimental variables as a function of water content of the emulsion at the critical heat flux (not a fixed heat flux) corresponding to the water content of each emulsion. Figure 9 shows the comparison of the average diesel burn-rate predicted by the model with the experimental average diesel burn rate values as a function of water content of the emulsion. The average burn rate of diesel decreases with increasing water content of the emulsion. This is due to the fact that with more water in the emulsion, there is less diesel separated from the same amount of emulsion. Thus, the diesel available for burning is provided at a slower rate from the emulsion layer. Hence, the diesel burn rate is lower. This effect counterbalances the fact that with increasing water fraction of the emulsion, the critical heat flux value will also increase, thus increasing the diesel burn rate.

Figure 10 shows the comparison of the burn time predicted by the model with the experimentally observed values of burn time for different water contents of the emulsion. The burn time decreases with increasing water content of the emulsion. This is caused by a combination of two opposing effects. First, with increasing water content, the average diesel burn rate decreases (as illustrated in Fig. 9), resulting in increase of total burn time. However, as the water content of the emulsion increases, for the same starting emulsion thickness, there is less

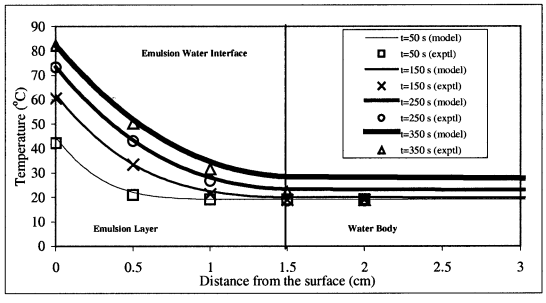


Fig. 8. Comparison of model predictions of temperature profiles with the experimentally recorded values of temperatures as a function of distance from the pool surface at various time intervals from start of heating.

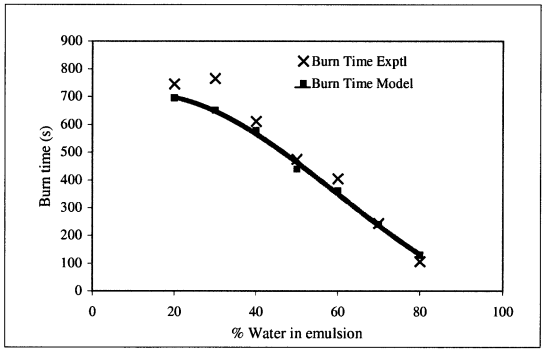


Fig. 10. Comparison of the burn time predicted by the model with the experimentally observed values of burn time as a function of water content of the emulsion at critical heat flux.

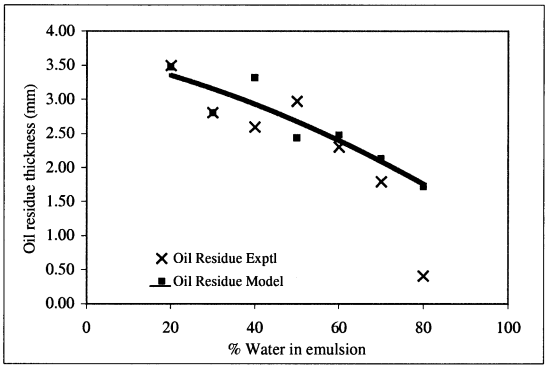


Fig. 11. Comparison of diesel residue thickness predicted by the model with the experimentally measured diesel residue thickness as a function of water content of the emulsion at critical heat flux.

diesel to be burned, resulting in reduced total burn time. The latter effect is more pronounced; therefore, the overall burn time decreases with increasing water fraction in the emulsion as seen in Fig. 10.

Figure 11 shows the comparison of diesel-residue thickness predicted by the model with the experimentally measured diesel residue thickness values as a function of water fraction of the emulsion. The residue thickness decreases with increasing water fraction in the emulsion. Again, this is caused by two different effects, both contributing to reduction in the residue thickness. First, with more water in the emulsion, there is less diesel to start with, given that the initial layer thickness is kept at 15 mm for all emulsions. Second, with increasing water fraction of the emulsion, the critical heat flux increases. Because the extinction occurs due to excessive heat loss to the water body, the emulsion thickness is smaller at extinction, therefore, the residue is actually smaller for emulsion having at higher water fraction.

It is clear from the results that, the model is capable of describing the significant processes involved in emulsion combustion adequately and thus is able to describe the experimental observations with good accuracy. It appears that such a model can provide additional insight before applying oil-spill combustion technique to real-life situations. It should be noted, however, that there is a lack of accurate property data.

## SUMMARY AND CONCLUSION

The paper presents a comprehensive mathematical model for the combustion of water-in-oil emulsion layers floating on top of a water body, as in case of in situ burning of oil spilled at sea that has formed an emulsion. The model was solved numerically by using a finite difference, pseudo-time algorithm. Laboratory scale burn experiments were conducted to establish a critical (i.e., minimum) heat flux value that needs to be incident on the emulsion surface so that a self-sustaining fire is produced. Among other variables measured and compared with model results are in-depth temperature profiles, emulsion separation time, burning rate, burn time, and residue thickness.

It was found that the time for emulsion separation increases with increasing water fraction of the emulsion at a constant heat flux value. The average diesel burning rate, total duration of the burn, and the volume of diesel remaining as residue decrease with increasing water content of the emulsion at the critical heat flux (corresponding to amount of water content in the emulsion). The mathematical model is capable of describing the significant processes involved in emulsion combustion adequately and thus is able to describe the experimental observations with good accuracy.

*Authors would like to thank Doug Walton of National Institute of Standards and Technology, US DOC, and Joe Mullin and Sharon Buffington of Mineral Management Service, US DOI, for the technical and financial support under grant no. 60NANBD0036.*

## REFERENCES

1. Fingas, M., and Laroche, N., *Introduction to In-Situ Burning of Oil Spills*, Spill Technology Newsletter, Environment Canada, Ottawa, Canada, 1990.
2. Walavalkar, A., and Kulkarni, A. K., *A Comprehensive Review of Oil Spill Combustion Studies*, Proceedings of the Nineteenth Arctic and Marine Oil Spill Program Technical Seminar, Environment Canada, Ottawa, Canada, 1996, p. 1081.
3. Guenette, C. C., Sveum, P., Bech, C., and Buist, I., *Studies of In-situ Burning of Emulsions in Norway*, Int'l Oil Spill Conference, American Petroleum Institute, Washington DC, 1995, p. 115.
4. Strom–Kristiansen, T., Lewis, A., Daling, P. S., and

Nordvik, A. B., *Demulsification by Use of Heat and Emulsion Breaker*, Proceedings of Eighteenth Arctic and Marine Oil Spill Program Technical Seminar, Environment Canada, Ottawa, Canada, vol. 1, 1995, p. 367.

5. Buist, I. A., Glover, N., McKenzie, B., and Ranger, R., *In-situ Burning of Alaska North Slope Emulsions*, Proceedings of the 1995 International Oil Spill Conference, American Petroleum Institute, Washington, DC, p. 139.
6. Thompson, C. H., Dawson, G. W., and Goodier, G. L., *Combustion: An Oil Spill Mitigation Tool*, PNL-2929, NTIS, US Department of Energy, Washington, DC, 1979, p. 53.
7. Guenette, C., Sveum, P., Buist, I., Aunaas, T., and Godal, L., *In-Situ Burning of Water-In-Oil Emulsions*, SINTEF Report STF21 A94053. Reprinted as MSRC Technical Report Series 94-001. Marine Spill Response Corporation, Washington, DC, 1994, p. 139.
8. Brzustowski, T. A., and Twardus, E. M., *Nineteenth Symposium (International) on Combustion*, The Combustion Institute, 1982, p. 847.
9. Putorti, A. D., Jr., and Evans, D., *Ignition of Weathered and Emulsified Oils*, Proceedings of the Seventeenth Arctic and Marine Oil Spill Program Technical Seminar, Environment Canada, Ottawa, Canada, vol. 1, 1994, p. 657.
10. Wu, N., Baker, M., Kolb, G., and Torero, J. L., *Ignition, Flame Spread and Mass Burning Characteristics of Liquid Fuels on a Water Bed*, Proceedings of Twentieth Arctic and Marine Oil spill Program Technical Seminar, Environment Canada, Ottawa, Canada, vol. 2, 1997, p. 769.
11. Arai, M., Saito, K., and Altenkirch, R. A., *Combust. Sci. Technol*. 71:25 (1990).
12. Garo, J. P., Vantelon, J. P., and Fernandez–Pello, A. C., *Twenty Fifth Symposium (International) on Combustion*, The Combustion Institute, 1994, p. 1481.
13. Hamins, A., Klassen, M. E., Gore, J. P., Fischer, S. J., and Kashiwagi, T., *Combust. Sci. Technol*. 97:37 (1994).
14. Pisarchik, M., Kocis, D., Walavalkar, A., and Kulkarni, A. K., *Effect of Temperature on Breaking of Water-in-Oil Emulsions*, Twentieth Arctic and Marine Oil Spill Program Technical Seminar, Environment Canada, Ottawa, Canada, 1997.
15. Buist, I., and McCourt, J., *The Efficacy of In situ Burning for Alaskan Risk Oils*, Final Report, S. L. Ross Environmental Research, Ltd., Ottawa, Canada, 1998.
16. Vargaftik, N. B., *Tables on the Thermophysical Properties of Liquids and Gases*, Hemisphere Publication Corporation, 2nd Ed., 1975, p. 695.
17. Arai, M., Saito, K., and Altenkirch, R. A., *Twenty Second Symposium (International) On Combustion*, The Combustion Institute, Seattle, WA, 1988, p. 1.

*Received 2 August 2000; revised 28 November 2000; accepted 19 December 2000*